

APPLICABILITY OF SURFACE WAVE METHOD TO BOUNDARY OF CUTTING AND FILLING OF RESIDENTIAL EMBANKMENTS

* Akinobu Ogasawara¹, Shota Hayashizaki², Shunzo Kawajiri³,
Takayuki Kawaguchi² and Dai Nakamura²

¹National Institute of Technology, Toyota College, Japan,
²Kitami Institute of Technology, Japan, ³Kyushu Institute of Technology, Japan.

*Corresponding Author, Received: 16 Feb. 2024, Revised: 04 July 2024, Accepted: 09 July 2024

ABSTRACT: In recent years, earthquakes have caused several types of damage to residential embankments. To assess the integrity of residential embankments and ascertain necessary countermeasures following ground disasters, it is crucial to accurately define the boundary of cutting and filling. Although surface wave methods nondestructively unveil the S-wave velocity V_s across a broad spectrum, there are currently no methods available to predict the boundary of cutting and filling based on V_s . In this investigation, surface wave measurements were conducted in an area thought to be an embankment, according to aerial topographic interpretation. The acquired V_s data were used to ascertain the soil characteristics of the unaffected residential embankment. Furthermore, the applicability of a method for predicting the boundary of cutting and fillings was examined. When the mode value of V_s within the embankment was selected as the threshold for the boundary of cutting and filling, some agreement was confirmed with the outcomes calculated through aerial topographic interpretation. In addition, a straightforward technique for calculating ground subsidence based on V_s was considered. It was found that it may be feasible to determine the estimated seismic settlement of residential levees swiftly and nondestructively throughout a sizable region. These results indicate that the use of the surface wave method has the potential to advance residential embankment health assessment systems.

Keywords: S-wave velocity, Residential embankment, Boundary of cutting and filling

1. INTRODUCTION

The 2018 Hokkaido Eastern Iwate earthquake struck at 3:07 a.m. on September 8, 2018, with a magnitude of 6.7 inland and an epicenter at a depth of approximately 37 km in the eastern Iwate region [1]. The highest magnitude of the earthquake was 7 on a Japanese scale in the city of Atsuma, which was located immediately above the epicenter. Multiple geo-disasters resulted from this earthquake [2]. Conversely, a massive calamity transpired in the Kiyota district of Sapporo City, about 50 km from the epicenter, due to ground shifting and collapse beneath a residential embankment constructed with volcanic ash [3,4]. The damaged land consisted of pyroclastic deposits (volcanic ash) that formed the surrounding slopes, and the valley plains, which had been utilized for agriculture in the 1970s, were filled with the material to create residential areas. In the Satozuka area, for example, a characteristic damage pattern was that the embankment of volcanic ash that had developed in the shape of a valley flowed along the slope of an old river due to liquefaction, and a large portion of the embankment spouted and poured out at the end of the constructed embankment. Although no significant horizontal displacement of the ground surface was observed, the liquefied soil layer generated a massive settlement of the ground surface, which lost its support and resulted in damage to several detached dwellings. When planning

countermeasures following a soil disaster, it is important to understand the damage mechanism based on the soil characteristics of the disaster area and to implement countermeasures according to the degree of damage to the houses. In some prior investigations, a straightforward technique for calculating post-seismic ground sinking using N values from common penetration tests has been considered. However, there is no instance in which the amount of ground sinking was determined using V_s data from the surface wave investigation.

In this study, we performed a surface wave investigation of a residential embankment where road subsidence was confirmed at the embankment boundary and around the embankment based on topographic and aerial photointerpretation to understand the soil properties and determine the applicability of the embankment boundary estimation method. Additionally, a simple technique for calculating the settlement amount using V_s data obtained from a surface wave method was investigated. In Kitami City, Hokkaido, the study site, no major ground disasters have occurred on residential embankments. However, a study is currently underway to predict changes in large residential levees. To provide complementary information to this survey, surface wave methods were conducted on residential embankments. A detailed evaluation of residential embankments in Kitami City was conducted using the results obtained

from a surface wave survey. These results provide important information for determining areas of high disaster risk and the scope of countermeasures. The results are reported below.

2. RESEARCH SIGNIFICANCE

Because the surface wave method is a nondestructive geophysical survey, it is impossible to directly obtain information on the soil properties of the target soil, unlike a borehole survey. Therefore, while borehole investigations are essential for evaluating the health of residential embankments, the V_s distribution obtained from surface wave methods can be effectively used as a primary screening method for deformations, enabling more efficient and effective selection of borehole investigation sites than is possible with conventional methods. Accordingly, the use of surface wave method has the potential to advance the health assessment system for residential embankments.

3. SURVEY METHOD AND TEST LOCATIONS

Figure 1 depicts the implementation of the surface wave method used in this study. Figure 2 shows a schematic of this idea. The surface wave method is a survey technique that allows one to ascertain the S-wave velocity of the soil by monitoring and examining surface waves (Rayleigh waves) that propagate near the soil surface [5]. Surface waves were produced when the ground surface was deliberately shaken with a hammer or wooden handle. The relationships between frequency and phase velocity were determined by Fourier analysis of waveforms recorded from these surface waves in the time domain, and a dispersion curve illustrating the relationship between phase velocity and frequency was produced by superimposing the results from all seismographs. Generally speaking, surface waves propagate at different depths depending on their frequency, with higher-frequency waves reflecting shallower bottoms and lower-frequency waves



Fig. 1. Status of surface-wave method

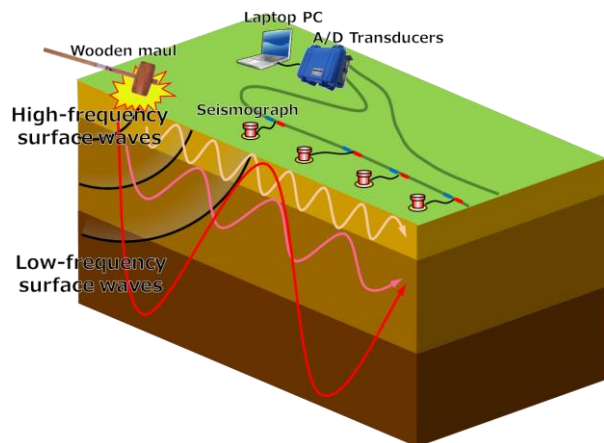


Fig. 2. Conceptual diagram of surface-wave method

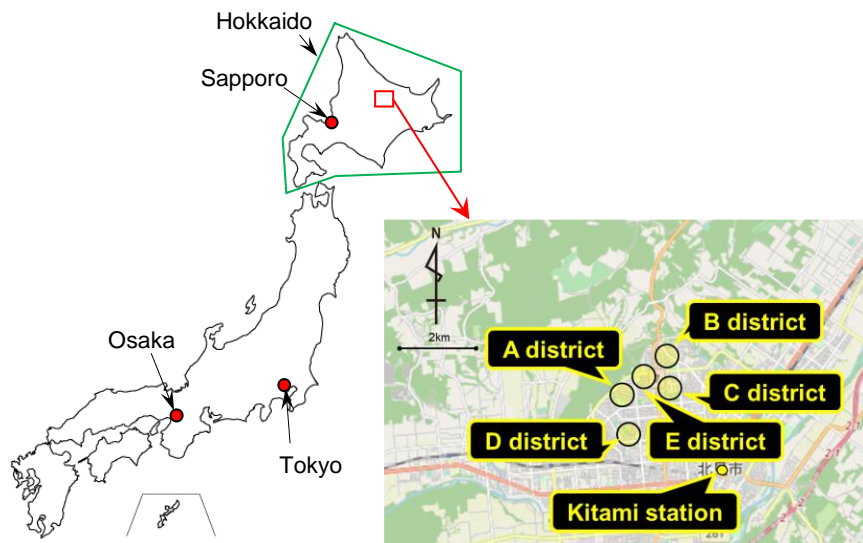


Fig. 3. District where surface-wave method was conducted in Kitami City, Hokkaido, Japan

reflecting deeper bottoms. For the analysis, an initial model was built using the empirical relationship that one-third of the wavelength correlates to depth, and the S-wave velocity structure that best fits the dispersion curve derived from the waveform records was estimated using inverse analysis. The analysis was performed for each seismograph according to its dispersion curve, and the S-wave velocity structure obtained for each seismograph was interpolated in the direction of the survey line to obtain the S-wave velocity (V_s) distribution. Because the shear stiffness, which represents the stiffness of the ground, is proportional to the square of V_s , an increase or decrease in V_s implies a greater or lesser degree of ground stiffness. A prior study found that V_s decreases at locations where the water content (saturation) within the embankment increases due to infiltration of rainfall. It has been stated that the water content within the embankment is determined by comparing V_s distributions when the change in the density of the embankment is thought to be minor [6]. Watabe and Sassa compared the results of borehole and surface wave methods for distinct geological formations that make up tidal flats. Consequently, they reported that the geologic structure and microtopography can be understood using the V_s distribution and applicability of the surface wave method [7]. In addition, Wijayanto et al. reported that seismic hazard assessment can be performed by determining the site conditions from the average shear wave velocity to an arbitrary depth[8]. The value of surface wave investigation in comprehending the characteristics of embankments

and natural soils has been demonstrated in numerous cases. This study benefits mitigate disasters and improve residential embankment maintenance systems.

Figure 3 depicts the locations where the surface wave method was applied in Kitami City, Hokkaido, Japan. The surface wave method was utilized to gather interpolative data to forecast fluctuations in the large-scale embankment in Kitami City, Hokkaido. Figure 4 displays the survey lines of the surface wave method based on the location. The figure shows the predicted fill area based on the difference in elevation between the old and updated topographic data. The survey lines were selected to be as complete as feasible to comprehend the soil quality in the locations where surface subsidence was confirmed and surrounding the cut boundary. The seismic excitation for the surface-wave method was a wooden rod (approximately 10 kg), and a seismograph (vertical motion) with a natural frequency of 4.5 Hz was used as the receiver. The number of points of seismic excitation was 24 for every seismic excitation, and the gap between the points was 2 m. The measurements were performed using a land streamer.

4. S-WAVE VELOCITY DISTRIBUTION OBTAINED FROM SURFACE WAVE METHOD

In the following, representative examples of S-wave velocity distributions obtained from surface wave method in various areas of Kitami City are presented, and a summary of the trends in S-wave

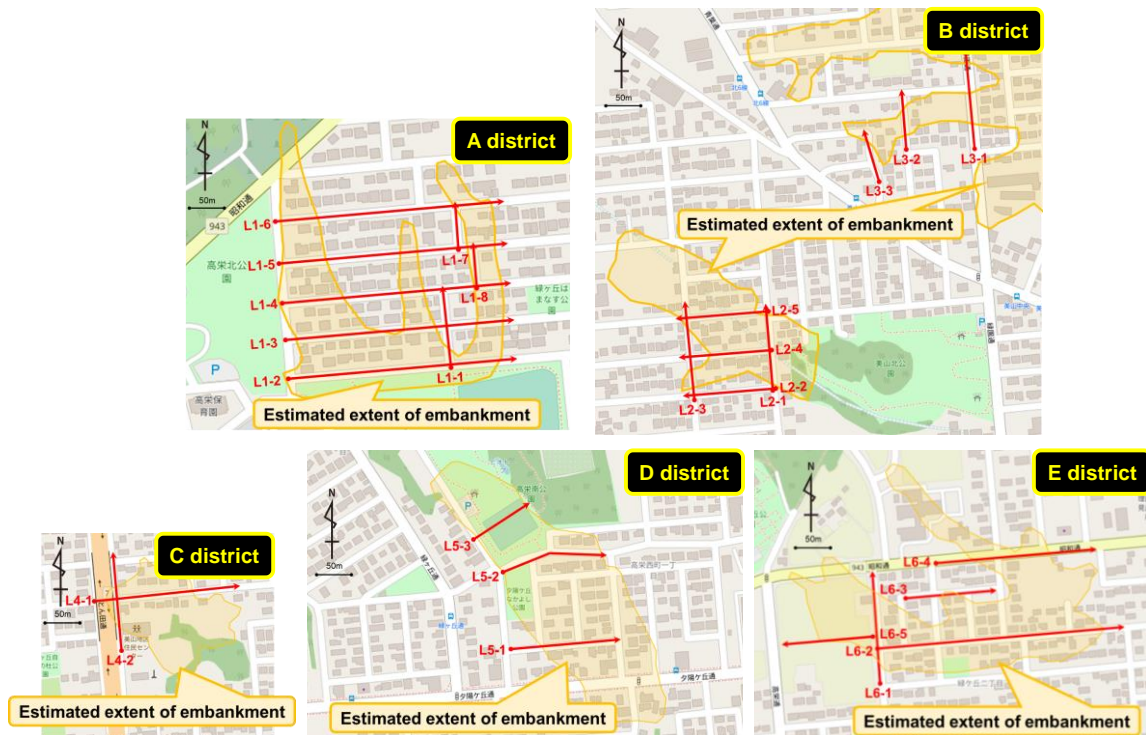


Fig. 4. Survey lines and estimated extent of embankment

velocity distributions in areas where surface subsidence, etc. has been confirmed and in the estimated extent of embankment is provided. Representative measurement lines and V_S ranges are displayed in the table.

4.1 A District in Kitami City

Figure 5 shows the results of L1-2, L1-3, and L1-5 as illustrations of the S-wave velocity (V_S) distributions acquired from the surface wave method. Table 1 displays each survey line and the range of V_S in A district. The results for L1-2 show that the measured lines were often within the estimated area of the embankment (Fig. 4). In the region $Y = 0-7$ m, there is an area of lower V_S of approximately $V_S = 100-140$ m/s. In the vicinity of $X = 90-110$ m and $Y = 2-4$ m, there is an area of reduced V_S of approximately $V_S = 140-160$ m/s. The area around $X = 90-110$ m was where road repairs have been carried out, and the V_S is quite high. In L1-3, V_S was relatively higher than that of L1-2, with $V_S = 120-160$ m/s at $Y = 0-7$ m. In L1-5, the V_S is comparatively higher than that of L1-2, with a $V_S = 120-160$ m/s at $Y = 0-7$ m. In L1-5, the area around the beginning and end of the survey line is the estimated extent of the embankment (Fig. 4), but there is no area with $V_S =$ approximately 100–140 m/s. In this area, the V_S is comparatively high compared to L1-2. The groundwater table may be high in L1-2 because the residential area in this area slopes to the south. Therefore, the V_S is regarded as being relatively low in areas where a high groundwater table is anticipated in the embankment area. No discernable subsidence of the ground surface was observed in A district.

4.2 B District in Kitami City

Figure 6 displays the results of L2-1, L2-3, and L2-4 as instances of the V_S distribution from the surface

Table 1. Survey line and range of V_S in A district

Survey line	Distance X (m)	Depth Y (m)	V_S Range (m/s)
L1-2	0-240	0-7	100-140
L1-2	90-110	2-4	140-160
L1-3	0-240	0-7	120-160
L1-5	0-240	0-7	140-180

wave method. Table 2 displays each survey line and the range of V_S in B district. In this area, sinking of the ground surface and the slope of the single-family houses were noted. In L2-1 and L2-4, the surveyed lines were mainly inside the estimated extent of the embankment (Fig. 4), and a low-velocity area with $V_S = 120-140$ m/s was observed in the area of $Y = 0-8$ m. In L2-3, the regions surrounding the start and finish of the measurement line were within the estimated extent of the embankment (Fig. 4).

Similar to L2-1 and L2-3, a low-velocity area ($V_S = 120-140$ m/s) is visible in the ranges of $X = 0-30$ m, 80-110 m, and $Y = 2-9$ m, respectively. In L2-4, the road surface sank at $X = 50$ m, and the low V_S area spread toward the depth at this point. In area L3, significant subsidence of the road surface was also noted in the area in which the V_S drop was localized. Although Kitami City has not previously experienced significant earthquake damage, the locations of the areas with severe road surface sinking and the localized region with V_S deterioration corresponded. Thus, it can be concluded that the surface wave method was also helpful in comprehending the soil characteristics of the distorted portions of the embankment prior to damage.

4.3 C District in Kitami City

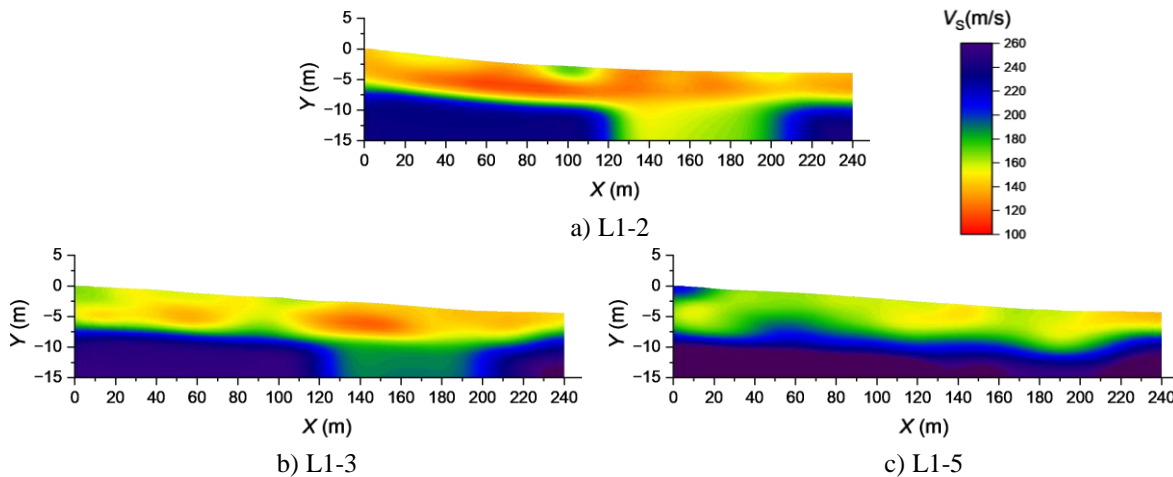


Fig. 5. Example of V_S distribution obtained from a surface wave method conducted in A district

Figure 7 shows the V_S distribution obtained from the surface wave method at this site. It can be seen that the difference in S-wave velocity is observed as the boundary at approximately $X = 130$ m at L4-1, and that the boundary position resulting from this difference in S-wave velocity and the estimated boundary of cutting and filling typically coincide. At L28-2, a zone of low V_S was spread over a considerable area, suggesting that the water table was high at this location.

4.4 D District in Kitami City

Figure 8 shows the V_S distribution obtained from the surface wave method at this site. The V_S at the end of L5-1 ($X = 150-160$ m) indicates that the thickness of the embankment was approximately 12 m. The V_S value in this area was not low, indicating that the quality of the embankment was guaranteed. The boundary of cutting and filling were visible at approximately $X = 45$ m, but the V_S distribution also demonstrated a drop in V_S from approximately $X = 45$ m, confirming the consistency of the boundary of cutting and filling. However, the V_S value at L5-3,

Table 2. Survey line and range of V_S in B district

Survey line	Distance X (m)	Depth Y (m)	V_S Range (m/s)
L2-1	0-110	0-8	120-140
L2-1	0-30	0-8	120-140
L2-3	80-110	2-9	120-140
L2-4	30-110	0-7	120-160

which is situated on the north side of the survey line, is comparatively low. This is due to the fact that there is a biotope in the park, and the water level in the embankment is rather high, which means that the V_S is lower, as expected. The findings of the surface wave survey at the location are regarded as a broad understanding of the local circumstances.

4.5 E District in Kitami City

Figure 9 illustrates the results for L6-1, L6-2, L6-3, and L6-4 as examples of the V_S distributions obtained from the surface wave method. Table 3 displays each survey line and the range of V_S in E

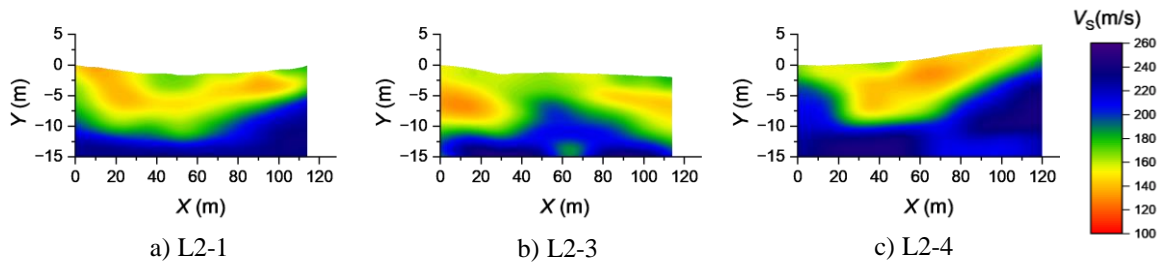


Fig. 6. Example of V_S distribution obtained from a surface wave method conducted in B district

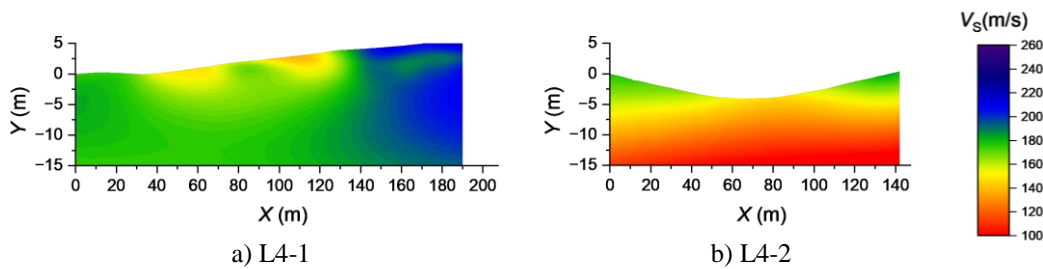


Fig. 7. Example of V_S distribution obtained from a surface wave method conducted in C district

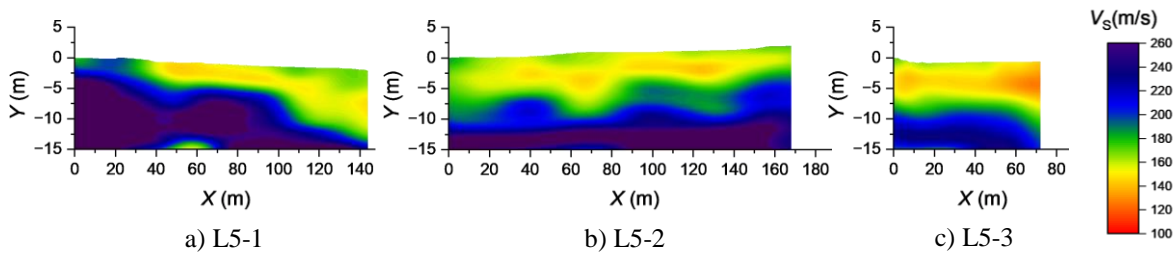


Fig. 8. Example of V_S distribution obtained from a surface wave method conducted in D district

district. The general trend is that the V_S zones with modest velocities (i.e., $V_S = 130\text{--}150$ m/s) are scattered within the predicted extent of the embankment. Moreover, at $X = 45\text{--}70$ m in L6-3, where ground deformation is very noticeable, a low-velocity area ($V_S = 100$ m/s) can be found. Consequently, it can be expected that the water level in the embankment is higher and the density of the embankment is lower. This result is consistent with the fact that repeated surface subsidence has occurred at this site and that the overburden has been repeated.

Near the endpoint of L6-2 at $X = 270\text{--}320$ m, the values of $V_S = 120\text{--}140$ m/s are scattered up to $Y = 10\text{--}20$ m. This area is estimated to match the fill thickness; however, the comparatively soft fill thickness near the end of the old stream is believed to be thicker than anticipated. At L6-4, a high-velocity zone of approximately $V_S = 180\text{--}260$ m/s was found on the starting side (i.e., $X = 0\text{--}50$ m). The findings are consistent with the estimated extent of the embankment and provide a clear picture of the local circumstances at the location.

5. METHOD FOR INVESTIGATING S-WAVE VELOCITY THRESHOLDS

In a surface wave method conducted after the earthquake in Sapporo, Hokkaido, Japan, the authors reported that the V_S decreased in the areas where the subsidence caused by the earthquake was significant, suggesting that the surface wave method is useful for determining soil properties in deformed areas. Furthermore, it was mentioned that the location of the fill boundary could be approximately estimated using the mode value of V_S in the fill in the V_S distribution found by the surface wave method conducted on a damaged residential embankment [9].

Figure 10 depicts the thresholds of the slope

Table 3. Survey line and range of V_S in E district

Survey line	Distance X (m)	Depth Y (m)	V_S Range (m/s)
L6-1	0–140	0–7	130–150
L6-2	270–320	10–20	120–140
L6-3	45–70	2–5	100–120
L6-4	0–50	0–15	180–260

boundary considered in this study and a typical V_S distribution reflecting the thresholds according to this method. The distance to boundary of cutting and filling estimated by this method was compared with the distance boundary of cutting and filling by an aerial topographic interpretation based on the 0 m line of the surface wave method.

Figure 11 presents the findings of a study on the applicability of a method for calculating the boundary of cutting and filling in an area for which no borehole data were available, based on the surface wave method applied to a residential embankment in Kitami City, which was not affected by the earthquake. In the case of Kitami City, where there is no borehole soil classification, the mode value of V_S , which is the least affected by increases in V_S due to recompaction for road repair and decreases in V_S due to the decrease in soil stiffness caused by seismic motion, was used as the threshold value for comparison. The procedure for determining the V_S mode value in a survey line without borehole data is as follows: First, the depth distribution of V_S at 2 m intervals in the survey direction (X-axis direction) is extracted from the V_S distribution, the depth at which V_S increases in the depth distribution at that point is determined (e.g., approximately 7 m in Figure 5), and the V_S within that depth and the length of the survey

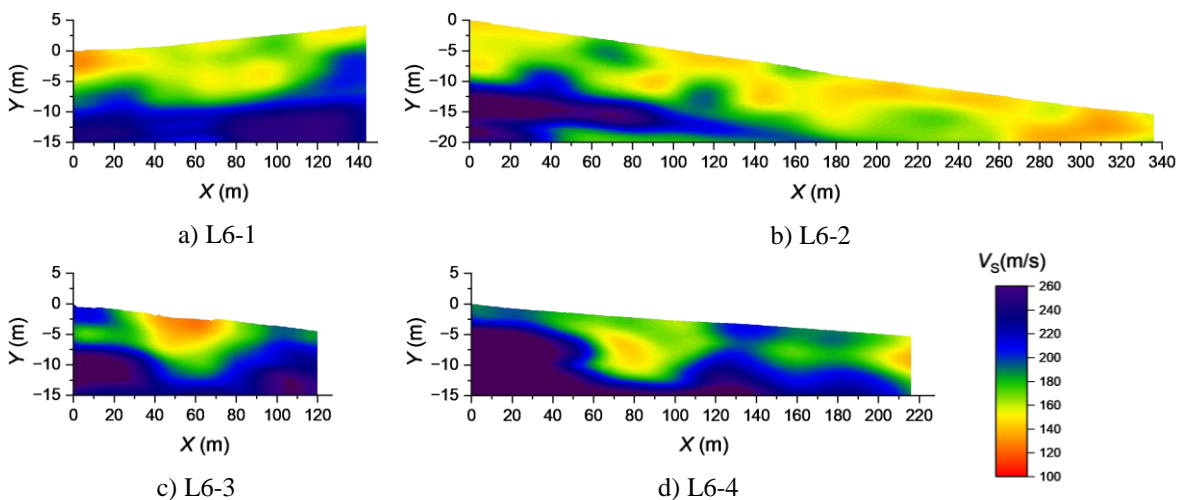


Fig. 9. Example of V_S distribution obtained from a surface wave method conducted in E district

line as V_S in the area of that depth and the length of the survey line were calculated as the mode value. In A and C districts, there are minor variations owing to the impact of smaller V_S in the region where the water table is predicted to be higher within the embankment area. Nonetheless, in districts B, D, and E, the boundary of cutting and fillings were typically distributed within ± 10 m. The aforementioned findings imply that it is possible to estimate the boundary of cutting and filling using the mode value of V_S , even in regions where borehole data are unavailable. In the future, it is necessary to increase accuracy by focusing on the age at which the embankment was created.

6. RELATIONSHIP BETWEEN S-WAVE VELOCITY AND GROUND SURFACE SUBSIDENCE

The aforementioned findings demonstrate that the S-wave velocity distribution acquired by the surface wave method can be used to identify a variety of post-earthquake ground characteristics, including the limits of cuts and fills and isolated low-velocity V_S zones. This benefit can be utilized to swiftly evaluate post-earthquake soil qualities to highlight regions that require care in the case of another tragedy caused by aftershocks, or as an indicator for prioritizing places where countermeasures should be implemented. In this study, we investigated the relationship between the S-wave velocity distribution and the amount of ground surface subsidence. There are multiple techniques for estimating the ground displacement during earthquakes. Tanabe et al. suggested a straightforward estimation equation (Eq. 1) for ground subsidence during an earthquake based on the sand layer thickness, maximum acceleration A , and sand layer mean N value as parameters [10]. Equations 2 and 3 are used to convert the N values and V_S used in the specifications for road bridges [11]. When a surface wave method was applied to a residential embankment in Kitami City, localized ground subsidence was confirmed in B and E districts. Assuming that this subsidence was caused by the Tokachi-oki earthquake in 2003, we compared the observed and estimated sinking using 130 gal measured at an observation station in Koen-cho, Kitami City, based on strong-motion records from the Japan Meteorological Agency [12].

Figure 12 displays the outcomes. Because the boundary of cutting and filling could be inferred by using the mode value of V_S , as previously indicated, the sand layer thickness at the subsidence point in Equation 1 was calculated from the V_S distribution, reflecting the mode value as a threshold value. The average value of V_S in the depth direction up to the sand layer thickness, calculated by the mode value, was used to determine the N value using Equation 3.

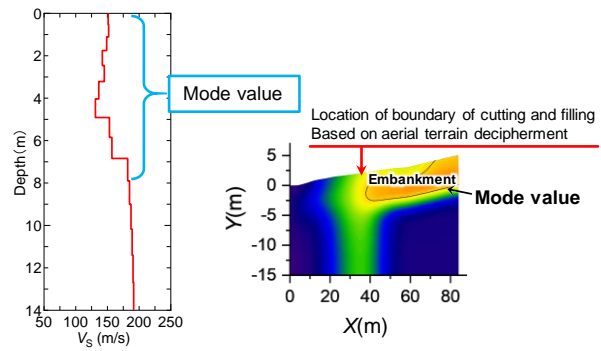


Fig. 10. Threshold determination method and typical S-wave velocity distribution reflecting the threshold

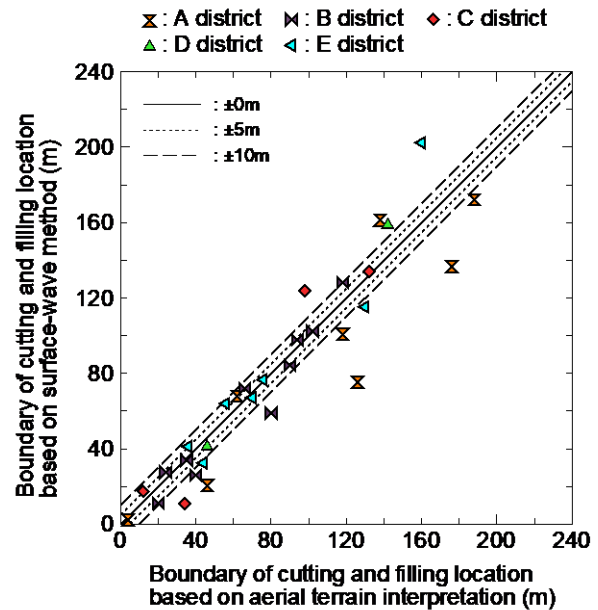


Fig. 11. Comparison of boundary of cutting and filling locations in Kitami City

The anticipated settlement based on the mean value of V_S was smaller than the measured settlement, whereas the distribution was typically within ± 50 cm at all measurement points. For the residential embankment in Kitami City, the thickness of the sand layer was determined from the mode value of V_S in an arbitrary depth direction because of the lack of borehole data, which may have led to a smaller predicted drawdown than the actual thickness of the embankment. These findings demonstrate that it is possible to obtain an approximate value for the seismic subsidence of the embankment under examination, albeit with an accuracy of ± 50 cm, by replacing V_S with the parameters of the current simplified subsidence estimation formula. Conventional surface wave methods capture a two-dimensional V_S distribution and determine soil parameters based on the relative change in V_S . Nonetheless, by substituting the parameters of the current simplified settlement estimation formula with V_S , an approximate value of the seismic settlement of

the embankment to be surveyed could be determined, albeit with an accuracy of ± 50 cm. However, because one of these characteristics has been replaced, it is important to consider ways to increase accuracy.

7. CONCLUSION

In this study, surface wave measurements were conducted on a residential embankment, and the method and applicability of predicting the boundary of the cutting and filling from the V_s were examined. Furthermore, correlations between the S-wave velocity distribution and ground subsidence of the ground surface were investigated. The conclusions are summarized as follows:

- (1) In the method for determining the boundary of cutting and filling from the V_s distribution acquired from the surface wave method, based on the mode value of V_s in the embankment as the threshold value, the values obtained some agreed with those calculated from aerial topographic interpretation.
- (2) Substituting the N value into the current empirical formula for estimating the seismic subsidence of the ground surface by V_s enables a quick and nondestructive determination of the approximate value of the seismic sinking of residential embankments over a wide region.
- (3) The use of the surface wave method has shown the potential to develop an evaluation system for the health of residential embankments.

8. ACKNOWLEDGMENTS

The survey was conducted with the cooperation of Mr. Masahiro Fukushima and Mr. Kiyohiko Shudo of the Kitami City Urban Construction Department. In addition, Dr. Hijiri Hashimoto of the Civil Engineering Research Institute for Cold Region advised us about the location and results of the survey.

9. REFERENCES

[1] The Headquarters for Earthquake Research Promotion., Evaluation of the 2018 Hokkaido Eastern Iburu Earthquake, 2018. https://www.static.jishin.go.jp/resource/monthly/2018/20180906_iburi_3.pdf.

[2] Ishikawa T., Yoshimi M., Isobe K., and Yokohama S., Reconnaissance Report on Geotechnical Damage Caused by 2018 Hokkaido Eastern Iburu Earthquake with JMA Seismic Intensity 7, Soils and Foundations, Vol. 61, No. 4, 2021, pp.1151-1171.

[3] Yamashita S., Ogawa K., Kawajiri S., Kawaguchi T., and Watanabe T., Liquefaction Characteristics of Residential Volcanic Soil Ground Suffered by 2018 Hokkaido Iburu Tobu Earthquake -

$$\text{Amount of subsidence (cm)} = 2.52 + 0.250 \frac{\text{Sand layer thickness (m)} \times \text{Maximum acceleration } A(\text{gal})}{\text{Sand layer } N \text{ value}} \quad (1)$$

$$\text{Cohesive soil } V_s = 100 N^{(1/3)} \quad (1 \leq N \leq 25) \quad (2)$$

$$\text{Sandy soil } V_s = 80 N^{(1/3)} \quad (1 \leq N \leq 50) \quad (3)$$

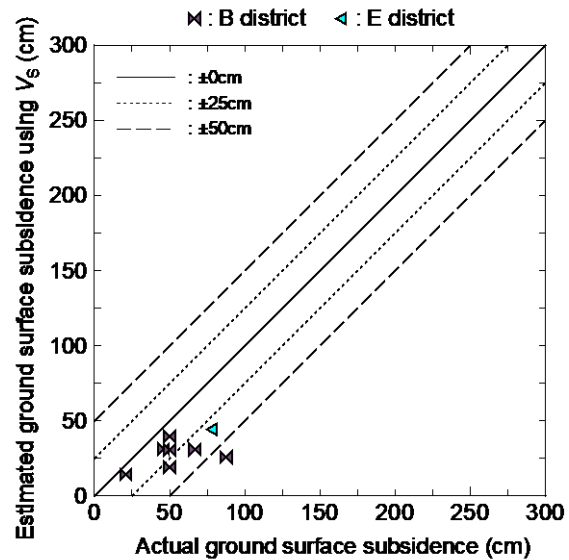


Fig. 12. Comparison of ground surface subsidence in Kitami city

Comparison with Agricultural Volcanic Soil Ground Suffered by 2003 Tokachi-oki Earthquake-, Japanese Geotechnical Journal, Vol. 14, No. 4, 2019, pp. 353-361.

[4] Watabe Y., and Nishimura S., Ground Movements and Damages in Satozuka District, Sapporo, due to 2018 Hokkaido Eastern Iburu Earthquake, Soils and Foundations, Vol. 60, No. 5, 2020, pp.1331-1356.

[5] Park C.B., Miller R.D., and Xia J., Multichannel Analysis of Surface Waves, Geophysics, Vol. 64, No. 3, 1999, pp. 800-808.

[6] Kawajiri S., Kawaguchi T., Hashimoto H., Tanaka Y., Nakamura D., and Yamashita S., Application for Surface-Wave Method to Property of Embankment, Japanese Geotechnical Journal, Vol. 13, No. 1, 2018, pp. 61-74.

[7] Watebe Y., and Sassa S., Application of MASW Technology to Identification of Tidal Flat Stratigraphy and Its Geoenvironmental Interpretation, Marine Geology, Vol. 252, 2008, pp. 79-88.

[8] Wijayanto., Mardiatno D., Daryono., Nehren U., Marfa M.A., Pramono S., Spatial Distribution of VS30 Based on MASW and Microtremor Inversion in Gunungkidul, Yogyakarta, International Journal of GEOMATE, Vol. 22 Issue 94, 2022, pp. 29-38.

[9] Kawajiri S., Ogasawara A., Kawaguchi T., Sasaki

- M., Sushida K., Yamashita S., S-Wave Velocity Profile of Residential Volcanic Soil Embankment Collapse Due To 2018 Hokkaido Iburi Tobu Earthquake, Japanese Journal of JSCE (Structural and Earthquake Engineering), Vol. 76, No. 4, 2020, pp. I_87-I_95.
- [10] Tanabe K., Takada S., Estimation of Earthquake Induced Settlements for Lifeline Engineerings, Japanese Journal of JSCE, Vol.1988, No.392, 1988, pp. 377-384.
- [11] Japan Road Association, Specifications for Highway Bridges Part V Seismic Design, 2017, pp. 69.
- [12] Ministry of Land, Infrastructure, Transport and Tourism, Strong Motion Observation Data, 2019. https://www.data.jma.go.jp/svd/eqev/data/kyoshin/jishin/1809060307_hokkaido-iburi-tobu/index.html.

Copyright © Int. J. of GEOMATE All rights reserved, including making copies, unless permission is obtained from the copyright proprietors.
